

On Gathering and Control of Unicycle A(ge)nts with Crude Sensing Capabilities

David Dovrat and Alfred M. Bruckstein, *Technion, Israel Institute of Technology*

A local rule of behavior for extremely simple unicycle agents has them gather and remain close to one another, without ever acquiring information on exact distances or bearings toward other agents.

The field of swarm robotics has emerged from the desire to harness the power of robust, decentralized, cost-effective, no single point of failure systems. *Rendezvous* (or the more general *gathering* problem) is one of the classic concerns of swarm robotics:¹ the ability to converge to a single or

confined set of configurations from a dispersed initial configuration. The *formation* problem is a natural extension of the gathering problem, where the set of configurations the agents converge to is a predefined shape. Another classic problem is *collective movement*, in which the swarm moves toward some desired goal.² Solutions to these problems differ by the level of sophistication required from the swarming agents to perform their tasks.

This work stems from a desire to manipulate a swarm of simple agents without explicit communication with any specific agent and without pre-labeling agents as leaders. Yotam Elor and Alfred Bruckstein³ demonstrated such capabilities in a scalar-field gradient climb, yet to prevent rendezvous at a single point in space, which would end the process, they added a random motion component, which would prove difficult to implement using real inertial robots.

Another way of preventing rendezvous is by gathering to a formation instead. Eric

Schoof and colleagues⁴ solved the formation and collective movement problems for single integrator agents, equipped with compasses, using bearing-only measurements. Shiyu Zhao and Daniel Zelazo⁵ achieved formation and collective movement for single integrator agents without requiring any information about the global frame, yet requiring relative position measurements. Both of these solutions to the formation problem trade off agent anonymity to pre-determine the desired formation, and both require the communication of specific control inputs to specific leader agents to control the scale of the formation achieved.

In another model, Ilana Segall and Bruckstein⁶ showed how a broadcast control, received by some agents, labels those agents as ad hoc leaders for the duration of receiving the broadcast signal, allowing the swarm to translate its location as long as any agent receives the control signal. When no agent receives an exogenous control signal, the model asymptotically converges to a rendezvous

point. This example trades off formation for leader agent anonymity.

Rodolphe Sepulchre and colleagues⁷ used relative heading and position measurements to make their agents circle a common center of rotation, form a balanced splay state formation, or move together in parallel, thus finding a balance between agent anonymity and formation while keeping a constant forward velocity, making their model fit for fixed-wing aircraft. However, incorporating relative heading into the swarming protocol requires sophisticated agents that can either measure other agents' relative heading or communicate their own global heading to other agents. Ronghao Zheng and Dong Sun⁸ presented models that require either bearing- or range-only measurements, requiring far less sophisticated agents to rendezvous, yet their models still require omnidirectional sensors. Our aims in considering simplified sensing are similar to those recently proposed by Melvin Gauci and colleagues,⁹ where the gathering problem is solved for agents with line-of-sight sensing.

Here, we present a decentralized, scalable, self-organizing swarm of anonymous unicycle type agents with a positive forward speed. The agents forming the swarm are severely limited in their sensing abilities, as they can make only a crude judgment on whether any other agents are in a sector in front of them or not. The agents are also memoryless and oblivious to a global frame of reference. This swarm of extremely simple agents is shown to solve the gathering problem, while managing to avoid rendezvous to a point and remain in a cohesive behavioral pattern once gathered, forming a rotating regular polygon in some instances. The swarm can also be induced to perform collective movement.

The Model

Simplicity is a key factor when designing swarming agents and is the main ingredient in the model proposed here.

We've based it on the popular *unicycle model*, which can be implemented using a variety of platforms, including wheeled vehicles subject to a nonholonomic constraint. The proposed model also enforces a forward motion speed greater than some defined positive parameter, allowing its implementation on platforms that have minimal velocity constraints, such as some fixed-wing drones. Sector visibility sensing, when compared to omnidirectional sensing, is quite straightforward to implement. Omnidirectional sensing is relatively difficult to achieve using onboard sensors—for example, a robot agent would have to have at least one wide-angle lens, and then would have to either do some computing to translate from image coordinates to real-world bearing or have an array of sensors and then stitch the sensors' outputs into a coherent snapshot of the current situation, requiring computational power, which isn't lightweight, low on power consumption, or cheap. None of these problems arise in a robot with sector visibility—one simple camera or sensor being enough—and only minimal computational power is required to translate the sensor output into an algorithm's input.

Unicycle Model

Agent i 's motion in the plane is governed by the equation

$$\begin{bmatrix} \dot{x}_i \\ \dot{y}_i \\ \dot{\theta}_i \end{bmatrix} = \begin{bmatrix} v_i \cos(\theta_i) \\ v_i \sin(\theta_i) \\ \omega_i \end{bmatrix}, \quad (1)$$

where $(x_i, y_i, \theta_i)^T$ are the agent's state, comprising agent i 's location, $p_i = (x_i, y_i)^T$, and orientation θ_i in an arbitrary global frame of reference. Here, v_i and ω_i are agent i 's control inputs, determining its speed and rotation rate, respectively.

The instantaneous center of rotation for agent i is denoted by c_i ,

$$c_i(t) = p_i(t) + \mathcal{R} \begin{bmatrix} -\sin(\theta_i(t)) \\ \cos(\theta_i(t)) \end{bmatrix},$$

where \mathcal{R} is the agent's trajectory's instantaneous curvature radius.

Sector Visibility

Consider a system of N agents, each equipped with a binary sensor able to detect only whether another agent is within a sector with visibility radius R_v and a central angle α in the direction the agent is facing. A graph representation of such a system, $\mathcal{G} = \{\mathcal{V}, \mathcal{E}\}$, can be constructed such that every agent in the system is represented by a vertex in the graph, and all agents within agent i 's sector of visibility have edges directed from them to agent i . The sensor output given to agent i is either "true" if the number of edges directed at agent i 's vertex in the underlying graph or v_i 's indegree $\deg^-(v_i)$ is greater than zero or "false" otherwise.

Controller

The unicycle agent with dynamics (Equation 1) is controlled by the following law:

$$\begin{bmatrix} v_i \\ \omega_i \end{bmatrix} = \begin{bmatrix} v \\ \frac{v}{\mathcal{R}(\mathcal{G}, i)} \end{bmatrix}, \quad (2)$$

where v is a positive constant, and $\mathcal{R}(\mathcal{G}, i)$ is a scalar function defined over the graph $\mathcal{G} = \{\mathcal{V}, \mathcal{E}\}$ such that

$$\mathcal{R}(\mathcal{G}, i) = \begin{cases} r & \text{if } \deg^-(v_i) = 0 \\ R & \text{otherwise.} \end{cases}$$

Here, $0 < r < R$ and $\deg^-(v_i)$ is the number of neighbors perceived by agent i , that is, the indegree of agent i 's vertex in the system's graph representation. The controller presented here is decentralized in the sense that every agent's behavior relies solely on the single agent's indegree, information that isn't shared with other agents. Scalability is a byproduct of this decentralization. Furthermore, in the controller's perspective, all agents

are anonymous, and the controller isn't affected by which edge, and therefore which agent, contributes to the indegree of any specific agent. The fact that only the indegree matters renders exact measurement of bearing angles and relative positions unnecessary, allowing the agents to be fitted with crude sensors, such as a single camera with a limited field of view and no depth perception. Additional sensors such as GPS or compasses are also unnecessary due to the fact that the controller doesn't have a global reference point or even a global direction reference, making the agents content in their obliviousness. Furthermore, the controller is stateless as only the current system state is used to resolve the value of $\mathcal{R}(\mathcal{G}, i)$, making all agents memoryless.

Beacon-Agent and Two-Agent Systems

Consider a system comprising one agent and one static beacon, located without loss of generality at $(0, 0)$ in the global frame. Other than being static, the beacon plays the role of an agent for all purposes. The agent turns with radius r when not observing the beacon, and R otherwise. We find interest in this rather basic scenario as it can be completely analyzed and is relatively easy to understand. Furthermore, the beacon-agent system analysis is the most basic building block for subsequent generalization.

Theorem 1

A system consisting of a beacon located at the origin and a single agent controlled by Equation 2 with visibility range $R_v \geq \|c_a(t_{initial})\| + R$ converges to a periodic orbit having a stationary center of rotation c_a and constant angular velocity $\dot{\theta}_a$ such that

$$\|c_a\| = \begin{cases} \leq r \cos\left(\frac{\alpha}{2}\right) & \text{for } 0 < \alpha < \pi \\ = 0 & \text{for } \alpha = \pi \\ \leq -R \cos\left(\frac{\alpha}{2}\right) & \text{for } \pi < \alpha < 2\pi \end{cases}$$

and

$$\dot{\theta}_a = \begin{cases} = \frac{v}{r} & \text{for } 0 < \alpha < \pi \\ \in \left[\frac{v}{R}, \frac{v}{r}\right] & \text{for } \alpha = \pi \\ = \frac{v}{R} & \text{for } \pi < \alpha < 2\pi \end{cases}$$

in finite time, where $(t_{final} - t_{initial}) \leq T(\|c_a(t_{initial})\|)$ and $T(x)$ is given by

$$T(x) = \begin{cases} \frac{2\pi r + \alpha(R-r)}{2\nu(R-r)\sin\left(\frac{\alpha}{2}\right)}x + \frac{R-r}{\nu}\tan\left(\frac{\alpha}{2}\right) + \frac{3\alpha R + (6\pi + \alpha)r}{\nu} & 0 < \alpha < \pi \\ + \frac{(2\pi + \alpha)r^2}{\nu(R-r)} + \frac{\alpha R + 2\pi r}{2\nu\sin\left(\frac{\alpha}{2}\right)} + \frac{\pi r^2}{\nu(R-r)\sin\left(\frac{\alpha}{2}\right)}, & \alpha = \pi \\ \left(\frac{(R+r)}{2\nu(R-r)}x + \frac{4r^2}{\nu(R-r)} + \frac{13R+12r}{2\nu} \right)\pi, & \alpha = \pi \\ \frac{2\pi r + \alpha(R-r)}{2\nu(R-r)\sin\left(\frac{\alpha}{2}\right)}x + \frac{R-r}{\nu}\tan\left(\frac{\alpha}{2}\right) + \frac{(2\pi + \alpha)R + 4\pi r}{\nu} & \pi < \alpha < 2\pi. \\ + \frac{2\pi r^2}{\nu(R-r)} + \frac{\alpha R + 2\pi r}{2\nu\sin\left(\frac{\alpha}{2}\right)} + \frac{\pi r^2}{\nu(R-r)\sin\left(\frac{\alpha}{2}\right)}, & \pi < \alpha < 2\pi. \end{cases}$$

Proof

A full analysis and calculation of the upper bound on the convergence time can be found in our technical report.¹⁰ For brevity, we present here only the outline of the proof. Given a single agent with $0 < \alpha < \pi$ controlled by Equation 2 and a beacon located at the origin and perceived as an agent by the single agent's sensors, if at time $t_{initial}$, $\|c_a(t_{initial})\| < r \cos\left(\frac{\alpha}{2}\right)$, then the system is periodic with

$$\dot{\theta}_a(t) = \frac{v}{r},$$

since the beacon is always out of the agent's view. Similarly, given a single agent with $\pi < \alpha < 2\pi$ and $R_v > R\left(1 - \cos\left(\frac{\alpha}{2}\right)\right)$ controlled by Equation 2, if at time $t_{initial}$, $\|c_a(t_{initial})\| \leq -R \cos\left(\frac{\alpha}{2}\right)$, the system is periodic with

$$\dot{\theta}_a(t) = \frac{v}{R},$$

since the beacon is initially inside the agent's sector of visibility and never leaves. These two cases are the only cases where the beacon is close enough to be detected by the agent, yet no switch in the turning radius ever occurs. Because $R_v \geq \|c_a(t_{initial})\| + R$, the beacon is neither always detected nor never detected in all other cases, and the agent necessarily reaches a point in time where the beacon rises over the agent's dawn horizon, meaning the beacon crosses into the agent's sector of visibility from the agent's left side. Figures 1a and 1b categorize the agent-beacon interaction into states, by the distance between the agent and

beacon on the beacon's rise over the agent's dawn horizon. The reason for this categorization is that the agent's trajectory pattern from beacon-rise to the next beacon-rise differs from state to state. Each state, except sink state B , has a transition to another state, and all states have a duration until the agent transitions onward. The sink state has a time span as well: the time it takes from the moment the agent first reaches the state until it locks into a periodic orbit.¹⁰ Figures 1c and 1d show the state machines depicting the convergence of a beacon-agent system to a periodic orbit with $R < 2r$ and $R \geq 2r$, respectively. Notice the existence of loops from state E to itself and between states A and C in Figure 1c. Both loops resolve, however. The E self-loop resolves in a transition to any other state in a time period affine in $\|c_a(t_{initial})\|$, and the $A \rightleftarrows C$ loop resolves in constant time, depending solely on the system parameters R, r, ν, α , ending in a transition to sink state B . The upper bound on the time it takes for the agent to settle in a periodic orbit around the beacon, $T(\|c_a(t_{initial})\|)$, is calculated by summing all state and loop durations.

Figure 2 shows NetLogo (<http://ccl.northwestern.edu/netlogo>) simulation runs of a single agent and a beacon scenario. The difference between the simulations, other than the initial conditions, is that the agents have different sensor span angles: $\frac{\pi}{3}$ in Figure 2a, π in Figure 2b, and $\frac{4}{3}\pi$ in Figure 2c. In Figure 2b, the signature spiral of the sink state B is clearly noticeable.

Theorem 2

The distance between two agents controlled by Equation 2 with $0 < \alpha < 2\pi$ and $R_v > \|p_1(t_{initial}) - p_2(t_{initial})\| + 4R$ becomes bounded in finite time such that

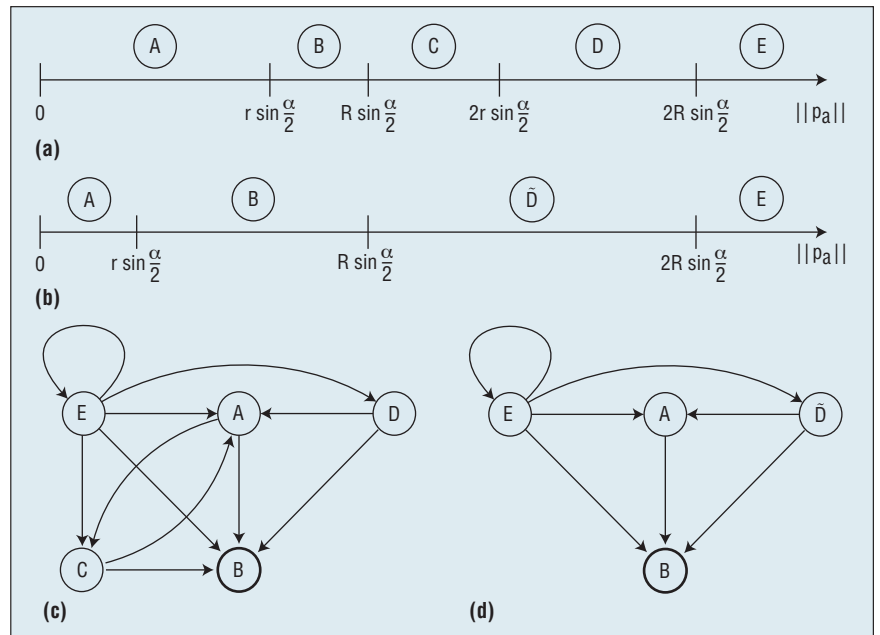


Figure 1. A state machine representation of the system's dynamics. (a) States A, B, C, D, E , where $R < 2r$. (b) States A, B, \tilde{D}, E , where $R \geq 2r$. (c) State machine for $R < 2r$. (d) State machine for $R \geq 2r$.

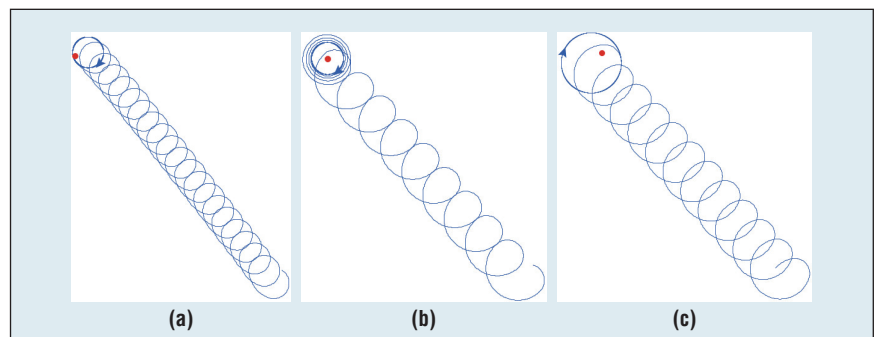


Figure 2. NetLogo simulation runs of a beacon and an agent with $R = 2r$. The dot represents the beacon, the arrowhead represents the agent: (a) $\alpha = \frac{\pi}{3}$, (b) $\alpha = \pi$, and (c) $\alpha = \frac{4}{3}\pi$.

$$\|p_1(t) - p_2(t)\| \leq \sqrt{\left(\frac{R \left(1 + 2 \cos \frac{\alpha}{2} \right) - r \left(1 - 2 \cos^2 \frac{\alpha}{2} \right)}{2 \sin \frac{\alpha}{2}} \right)^2 + \left(R + r \cos \frac{\alpha}{2} \right)^2} + (R - r) + 2R.$$

Proof

The theorem statement is a direct result of a geometric calculation.¹⁰

The upper bound in the previous result can be considerably shrunk, given the agents have opposite orientation at some point in time. Using the result

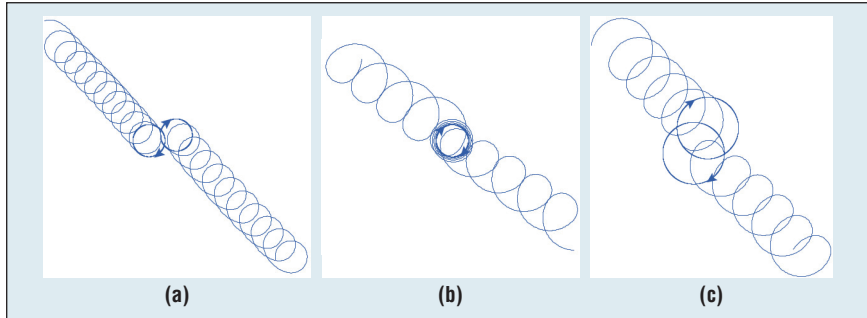


Figure 3. NetLogo simulation runs of a two-agent system with $R = 2r$: (a) $\alpha = \frac{\pi}{3}$, (b) $\alpha = \pi$, and (c) $\alpha = \frac{4}{3}\pi$.

$$\dot{\theta}_a = \begin{cases} \frac{v}{r}, & 0 < \alpha < \pi \\ \in \left[\frac{v}{R}, \frac{v}{r} \right], & \alpha = \pi \\ \frac{v}{R}, & \pi < \alpha < 2\pi. \end{cases}$$

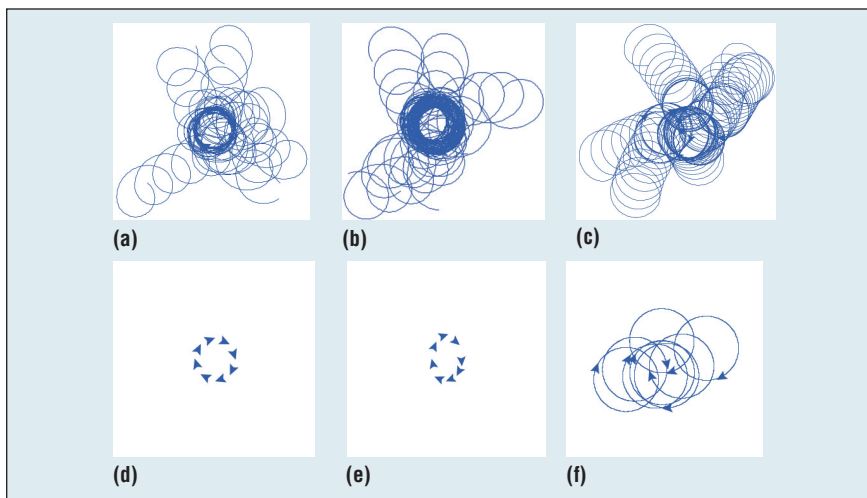


Figure 4. NetLogo simulation with eight agents with different α values. Subfigures (a), (b), and (c) show the cohesive behavior as the agents come closer together, while Subfigures (d), (e), and (f) show snapshots of the agent's configuration after gathering: (a) $\alpha = \frac{\pi}{4} = \frac{2\pi}{8}$, (b) $\alpha = \frac{\pi}{6}$, (c) $\alpha = \pi$, (d) $\alpha = \frac{\pi}{4} = \frac{2\pi}{8}$, (e) $\alpha = \frac{\pi}{6}$, and (f) $\alpha = \pi$.

obtained in Theorem 1, a tighter bound on the distances between agents in a two-agent system is presented.

Theorem 3

In a system consisting of two agents controlled by Equation 2 with $0 < \alpha < 2\pi$, if at time t_0 , $\cos(\theta_1(t_0) - \theta_2(t_0)) = -1$ and $R_v > \|c_1(t_0) - c_2(t_0)\| + 2R$, then for $t \geq t_0 + T_{total}(\|c_2(t_0) - c_1(t_0)\|)$, where $T_{total}(x)$ is affine in

x , the system converges to a configuration where both agents' centers of rotation are stationary and

$$\|c_1(t) - c_2(t)\| \leq \begin{cases} 2r \cos\left(\frac{\alpha}{2}\right), & 0 < \alpha < \pi \\ -2R \cos\left(\frac{\alpha}{2}\right), & \pi \leq \alpha < 2\pi. \end{cases}$$

In addition, the agents' angular velocity remains constant and common to both agents, $\dot{\theta}_1(t) = \dot{\theta}_2(t) = \dot{\theta}_a$,

Proof

If $\cos(\|\theta_1(t_0) - \theta_2(t_0)\|) = -1$, then the agents get into and out of each other's sector of visibility at the same time, creating point symmetry at $b = \frac{p_2(t) - p_1(t)}{2}$ with regard to the agent's trajectories. Point b is therefore stationary, and since the agents can't measure distances, detecting point b is equivalent to sensing the other agent. Invoking Theorem 1 for each of the agents with point b as the beacon defines $T_{total}(x)$, with $x = \|c_i(t_0) - b\|$, concluding this proof.

Through observations, we have noticed that in the two-agent system, the agents tend to synchronize their orientations to face opposite directions, and the following conjecture is made.

Conjecture 1

A two-agent system controlled by Equation 2, with $0 < \alpha < 2\pi$, converges in finite time to a periodic orbit such that both agents rotate in a circular pattern with a common, invariant radius R , around stationary centers of rotation, such that

$$\|c_1(t) - c_2(t)\| \leq \begin{cases} 2r \cos\left(\frac{\alpha}{2}\right) & 0 < \alpha < \pi \\ -2R \cos\left(\frac{\alpha}{2}\right) & \pi \leq \alpha < 2\pi \end{cases}$$

and

$$R = \begin{cases} r & 0 < \alpha < \pi \\ [r, R] & \alpha = \pi \\ R & \pi < \alpha < 2\pi. \end{cases}$$

Figure 3 shows NetLogo simulations of a two-agent system with different sensor span angles. Notice that although it starts with random orientations, the agents face opposite directions by the time the snapshots were taken.

N-Agent Systems

By observing numerous simulations of the model presented here, such as in Figure 4, the following conjectures are made based on the gathering behaviors observed.

Conjecture 2

A system of $N \geq 2$ agents controlled by Equation 2 with $0 < \alpha < \pi$ converges in finite time to a cohesive behavior in which every agent's trajectory intersects another agent's trajectory at least once every $\frac{2\pi R}{v}$ time period.

Conjecture 3

A system of $N \geq 2$ agents controlled by Equation 2 with $\alpha = \frac{2\pi}{N}$ converges to a regular polygon periodic orbit.

Collective Movement

Four methods of controlling the swarm presented here can be divided into two categories, with the first taking advantage of the swarm's scalability and gathering features. By either introducing new agents that don't adhere to the swarming protocol, as seen in Figure 6b, or abducting agents from the swarm, as seen in Figure 5d, the swarm is compelled to gather near the uncooperative leaders. The second category takes advantage of the fact that agent speed doesn't factor in the swarming protocol. By changing agent speed according to data acquired by additional sensors, control over the swarm's location can be added as a layer on top of the gathering protocol. In Figure 5e, the agents are assumed to be equipped with compasses. An azimuth is broadcast to all agents, yet each agent has a small probability ($P = 0.3$) to receive

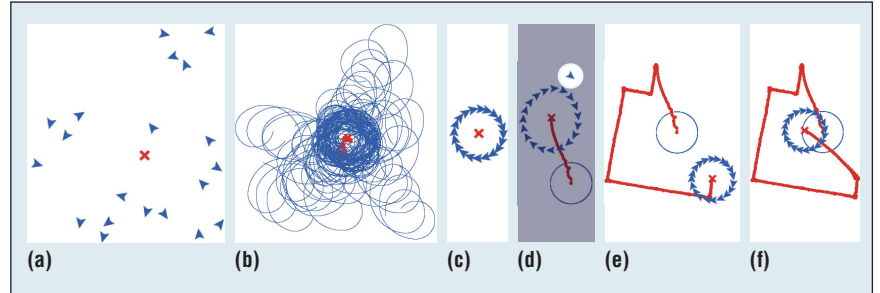


Figure 5. A NetLogo simulation with 20 agents with $\alpha = \frac{\pi}{10}$ illustrating collective movement. The geometric mean of agent's locations is marked by x . (a) Initially, all agents are scattered on the plane. (b) Left to their own devices, the agents gather. (c) The agents synchronize their phase towards a circular formation while gathering in accord with Conjecture 3. (d) Taking direct control over one of the agents and moving it to an arbitrary location (emphasized), the swarm follows the abducted leader. Notice the trace of the orbit achieved in Figure 5c. (e) Relinquishing control over the abducted agent, it returns to the fold. By broadcast control with 0.3 reception probability, the swarm is then induced to move south, west, south, east, then north. (f) Introducing a potential field instead of the broadcast signal, the swarm performs a gradient climb until reaching the local maximum, where it settles to a periodic orbit around a stationary point.

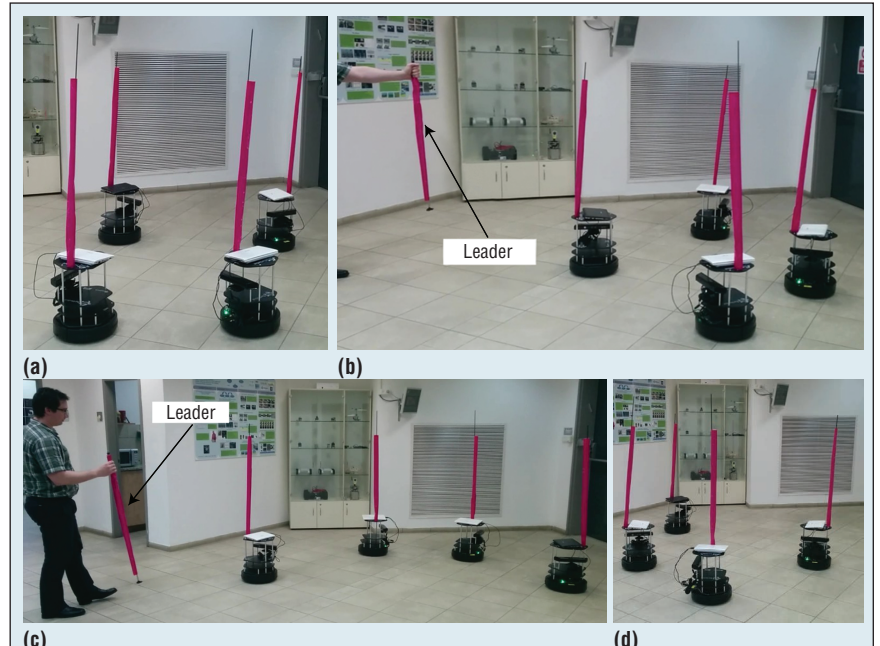


Figure 6. A swarm of TurtleBot2 platforms manipulated by an introduced leader. (a) Starting at scattered initial locations, the agents gather in a semicircular dynamic formation. (b) A leader agent is introduced to the swarm. (c) The swarming agents, true to their protocol, follow the leader. (d) Once removed, the leader agent no longer influences the swarm and the swarm returns to its cohesive behavior in a new location.

the transmission. Upon receiving the transmission, the agent becomes an ad hoc leader for some time, during which the leader alters its speed by $\gamma \sin(\alpha_c - \alpha_s)$, where γ is a gain parameter, α_c is the broadcast azimuth, and

α_s is the agent's heading. In Figure 5f, the agents are assumed to be equipped with sensors that sample a potential field at their immediate locations. In the example, the swarm climbs up the potential field $\varphi(x,y) = C - \sqrt{x^2 + y^2}$,

THE AUTHORS

David Dovrat is a research fellow at the Technion. His research interests include swarm robotics, autonomous vehicles, and real-time embedded systems. Dovrat received an M.Sc. in autonomous systems and robotics from the Technion Autonomous Systems Program (TASP). Contact him at dave.dovrat@gmail.com.

Alfred M. Bruckstein is the Ollendorff Chair in Science and professor in the computer science department at the Technion. His research interests include swarm robotics, image and signal processing, analysis and synthesis, pattern recognition, and various aspects of applied geometry. Bruckstein received a PhD in electrical engineering from Stanford University. Contact him at freddy@cs.technion.ac.il.

where C is an arbitrary constant, to its maximal value at the origin by altering each agent's speed by $-\gamma\varphi(x, y)$. Both methods in the speed-altering category cause agents that are closer to the desired translation direction to move slower than agents further away, resulting in a pull effect from slower agents and a push effect from faster agents.

Four-Agent System Experiment

Figure 6 shows an implementation of the presented model using TurtleBot2 platforms (www.turtlebot.com). Though equipped with a Kinect (with $\alpha = 62^\circ$) and a netbook running ROS (www.ros.org), the swarming protocol implementation uses only the RGB camera on the Kinect and could do with far less computational power than the netbook provides. The turtles are shown to converge twice, first when gathering from initial locations and once more when the interference of the leader agent is removed, in accord with Conjecture 2.

The decentralized model presented here is shown to be a scalable, self-organizing swarm of anonymous unicycle type agents that solves the gathering problem and, in some particular cases, the formation problem to a rotating regular polygon. The model requires the agents to have only limited sensing abilities, which enable the agents to make a crude, binary judgment on the existence of any

other agents in the sector in front of them by utilizing limited computation power and without any knowledge of a global frame of reference. The simplicity of the agents allows for a cost-effective implementation of the model, since the use of sophisticated equipment is rendered unnecessary. Possible methods for controlling the swarm's location show through example that the presented protocol could find use in simplifying control over a swarm by abducting or introducing a single agent and letting the rest follow, or by controlling the swarm as a unit by broadcasting a single datum. The presented swarm is also shown to be capable of finding a local maximum in a collectively sampled scalar field. Current research efforts are aimed at fully understanding the orientation synchronizing mechanism observed. Understanding this mechanism is key to a full analysis of the gathering and formation of regular polygons in the N -agent case and could prove useful in the analysis of future models based on the model presented here. Obstacle avoidance hasn't been covered in this work, yet the TurtleBot2 experiment presented has incorporated obstacle avoidance by adding range sensors, without hindering the swarm's gathering nature. □

References

1. N. Gordon, I.A. Wagner, and A.M. Bruckstein, "Gathering Multiple Robotic A(ge)nts with Limited Sensing Capabilities," *Ant Colony Optimization and Swarm Intelligence (ANTS 04)*, LNCS 3172, M. Dorigo et al., eds., Springer, 2004, pp. 60-87.
2. I. Navarro and F. Matía, "An Introduction to Swarm Robotics," *ISRN Robotics*, 2013; doi:10.5402/2013/608164.
3. Y. Elor and A.M. Bruckstein, "Robot Cloud Gradient Climbing with Point Measurements," *Theoretical Computer Science*, vol. 547, 2014, pp. 90-103.
4. E. Schoof, A. Chapman, and M. Mesbahi, "Bearing-Compass Formation Control: A Human-Swarm Interaction Perspective," *Proc. Am. Control Conf.*, 2014, pp. 3881-3886.
5. S. Zhao and D. Zelazo, "Bearing-Based Formation Maneuvering," *Proc. IEEE Int'l Symp. Intelligent Control (ISIC)*, 2015, pp. 658-663.
6. I. Segall and A.M. Bruckstein "On Stochastic Broadcast Control of Swarms," *Swarm Intelligence (ANTS 16)*, LNCS 9882, M. Dorigo et al., eds., Springer, 2016, pp. 257-264.
7. R. Sepulchre, D.A. Paley, and N.E. Leonard, "Stabilization of Planar Collective Motion with Limited Communication," *IEEE Trans. Automatic Control*, vol. 53, no. 3, 2008, pp. 706-719.
8. R. Zheng and D. Sun, "Multirobot Rendezvous with Bearing-Only or Range-Only Measurements," *Robotics and Biomimetics*, 2014; doi:10.1186/s40638-014-0004-5.
9. M. Gauci et al., "Self-Organized Aggregation without Computation," *Int'l J. Robotics Research*, vol. 33, no. 8, 2014, pp. 1145-1161.
10. D. Dovrat and A.M. Bruckstein, *Gathering & Collective Movement of Unicycle A(ge)nts with Crude Sensing Capabilities*, tech. report CIS-2017-02, Computer Science Dept., Technion, 2017.



Read your subscriptions
through the myCS
publications portal at

<http://mycs.computer.org>